

# Stochastic energy sink in a low-dimensional Hamiltonian system

V.N. Pilipchuk

*Wayne State University*

*e-mail: pilipchuk@wayne.edu*

Keywords: soft-wall billiards energy absorber energy harvester

**Abstract** A few-degrees-of-freedom applications to the design of macro-level Hamiltonian model exhibiting one energy absorbers, harvesters, and energy directional long-term trends in energy absorbing materials are discussed. exchange flows is introduced. The model includes a massive potential well - a container with one or few relatively light non-interacting particles - attached to a linearly elastic spring. No phenomenological dissipation is imposed, nevertheless, due to a similarity of the container shapes to typical stochastic soft-wall billiards, the energy is transferred from the container (donor) to the inner particles (acceptor) in almost irreversible way during physically reasonable time intervals. The potential well is introduced in such a way that, in the rigid-body limit, it resembles either Sinai billiards or the so-called Buminovich stadiums as the main geometrical parameter of the well switches its sign. In particular, using the nonlinear normal mode stability concept reveals conditions of stochasticity and determines the analogy with the dynamic properties of billiards. Possible

## I. INTRODUCTION

Modeling physical mechanisms of nonreciprocal energy exchange between coupled oscillatory subsystems represents a fundamental interdisciplinary problem. In particular, it may occur when designing molecular structures with desired *targeted energy transfer* properties [1], [8], [9], vibrational energy harvesters [3], [5], or mechanical energy absorbers for controlling the structural dynamics [15]. In the latter case, the intent is to create a relatively light device irreversibly absorbing the energy from the main structure. Since the Poincaré recurrence theorem prohibits such effects to occur within the class of conservative systems, the irreversibility is imposed phenomenologically using the conventional viscous damping. The core of such studies is therefore analyses of the resonance dynamics with the goal to intensify the en-

energy flow in a certain direction. The main problem is due to the fact that directions of resonance energy flows depend upon initial dynamic states. Therefore, stochasticity and ergodicity effects, allowing the system to ‘forget’ its initial states quickly enough, must be of interest in this case. Furthermore, we show below that such dynamic properties generate thermalization and dissipation, and thus irreversibility effects even when any phenomenological dissipation is absent at all. Note that either direct phenomenology or statistics of *large systems* are usually involved for modeling the dissipation [18], [6]. The present work however deals with the class of low-dimensional autonomous Hamiltonian systems whose irregular stochastic dynamics are caused by nonlinearities. A complete overview of this area, which has been under study for quite a long time, is rather outside the scope of the present work. Let us mention nevertheless that the corresponding phenomena may have very different physical nature. For instance, nonlinearities dictating the geometry of resonance manifolds, spectral overlaps, and modal interactions of the resonance dynamics were expected to generate thermalization effects in the Fermi–Pasta–Ulam (FPU) numerical test [16], [17]. It was found though that the FPU multiple degrees-of-freedom nonlinear chain model possesses certain properties of integrable systems yet with

a very complicated quasi-periodic behavior. An alternative class of models emerged from the theory of billiards [13], [2]. The billiard nonsmooth dynamics are quite opposite to the resonance quasi harmonic dynamics and therefore usually described in a different way through the discrete time mapping. Although trajectories of particles may be geometrically simple inside billiard domains, conditioning collisions of particles with billiard walls may appear to be quite complicated [12].

The present approach is two-fold. On one hand, we essentially employ the analogy with classical billiards for physical interpretations as soon as the soft-wall potential container of the present model can degenerate into two different basic types of billiards in the rigid-body asymptotic limit. On the other hand, we apply some analytical and numerical tools of smooth dynamics in order to determine conditions of stochasticity. The goal is to illustrate the possibility of a few degrees-of-freedom ‘energy sink’ within the class of Hamiltonian systems. Note that Poincaré recurrence is theoretically inevitable in such case, however, we show that its time span extends far beyond any natural time intervals of the system. In our case, *the effect is due to specific shapes of the soft-wall container*, represented by the moving potential well; see Figs.1 and 2. Although smooth potentials

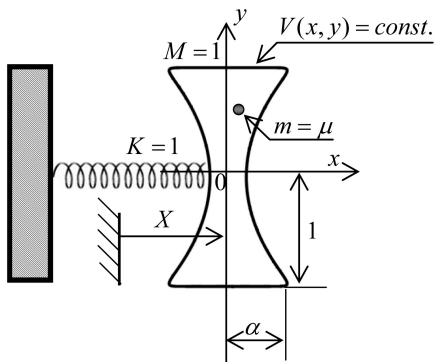


FIG. 1. A massive potential container oscillating with one small particle inside ( $k = 1$ ), which is interacting with potential walls of different ‘stiffness’ and contour shapes; see Fig. 2.

are shown, the physical justification of the results can be found within the theory of typical rigid-wall billiards, where the thermodynamic properties are associated with ergodicity and positive Lyapunov exponents due to the scattering effect of boundaries [13]. Few decades ago it was also found that the presence of convex scatters is not necessary for generating the dynamic stochasticity. The corresponding billiard shapes resemble stadium fields and are known as Buminovich stadia [2]. For that reason, the present model is developed in such a way that, in the rigid-body limit, it can degenerate into one or another type of billiards when changing the sign of the main parameter of the potential well,  $\beta$ ; see expression (1) below. Finally, the main specific of the present modeling is

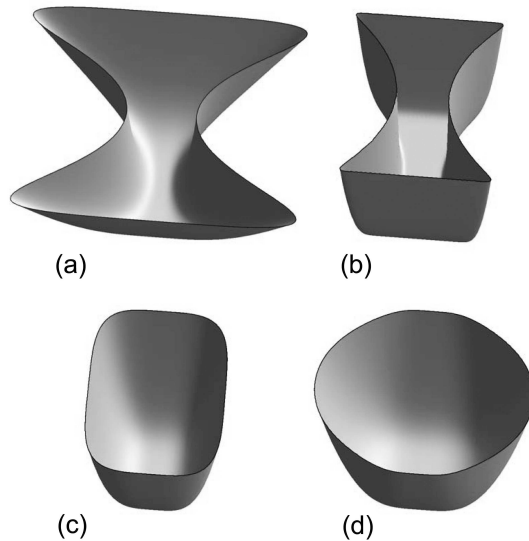


FIG. 2. Different shapes of the potential container obtained for  $\alpha = 1/2$  and  $\gamma = 1.0$ , and the following wall’s stiffness ( $n$ ) and contour’s curvature ( $\beta$ ) parameters: a)  $n = 2$ ,  $\beta = 0.3$ ; b)  $n = 10$ ,  $\beta = 0.3$ ; c)  $n = 2$ ,  $\beta = 0.0$ ; and d)  $n = 2$ ,  $\beta = -0.3$ .

that the soft-wall potential container possesses a finite mass attached to a linearly elastic spring and thus can dynamically interact with the contained particles creating two-way energy exchange flows. Nevertheless, the main trend of the energy exchange is shown to be one-directional. A brief physical explanation is that vibrations of the massive potential container are quasi regular, while the dynamics of relatively light particle(s) inside the container are quasi stochastic. Also, while the container’s motion is one-dimensional, the particle(s) path covers two-dimensional domains. Such specifics create

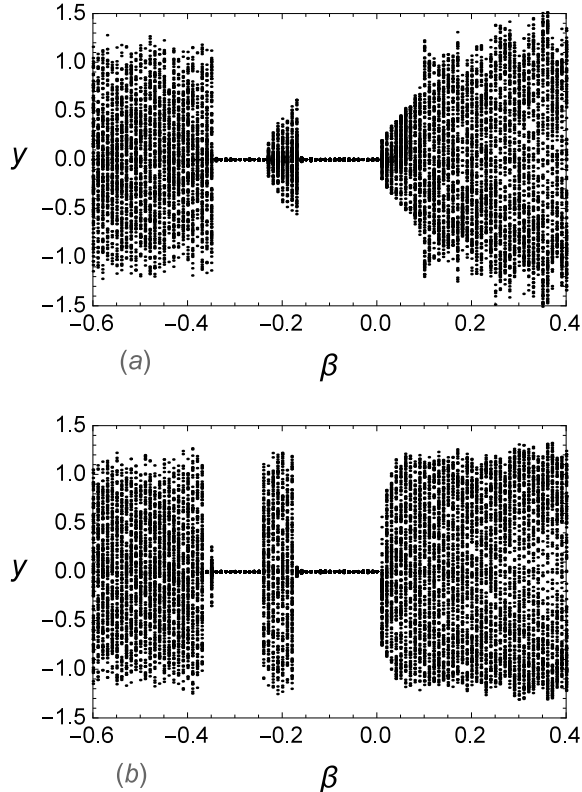


FIG. 3. Bifurcation diagrams revealing irregular stochastic motions in different negative and positive intervals of the curvature parameter  $\beta$  for a)  $n = 2$  - softer walls and b)  $n = 10$  - stiffer wall containers;  $\alpha = 1/2$ ,  $\gamma = 1.0$ .

different mechanisms for different directions of the energy exchange in such a way that one of the directions becomes dominant.

## II. MODEL DESCRIPTION

The model is illustrated in Fig.1, where a massive harmonic oscillator  $M$  represents a two-dimensional container described by the potential energy  $V = V(x, y)$ . The container is shown by a typical level line of the potential

energy in the non-inertial Cartesian frame  $xy$  associated with the axes of symmetry of the potential well. The container includes  $k$  relatively light non-interacting particles of the total mass  $m \ll M$ , which is driven by its interactions with the potential walls as the container is given some initial energy. The total mass of particles is fixed while their number can be different so that  $\mu = m/k$  is a mass of each particle. A practical macro-level design for such a model may include  $k$  parallel containers in order to exclude interactions between the particles. As mentioned in Introduction, we intentionally assume no phenomenological dissipation in the system, in other words, the total energy of the oscillator with particles is conserved, and thus the system is Hamiltonian. Therefore, elastic collisions with the container's walls affect also the dynamics of container however in a less dramatic way. The presence of such a feedback, which is usually ignored in statistical studies, represents a key assumption of the present work whose purpose is the analysis of recurrence effects versus contour shapes of the potential energy. Another difference with the typical statistical studies of non-interacting gas models is that the number of particles,  $1 \leq k \leq 5$ , is rather insufficient to provide the statistics of large numbers. Assuming no gravity is present, the potential

energy is modeled with the function

$$V = \frac{\gamma}{2n} \left[ \left( \frac{x}{\alpha + \beta(y^2 - 1)} \right)^{2n} + y^{2n} \right] \quad (1)$$

As follows from Fig.2, the phenomenological expression (1) provides a convenient way to modeling qualitatively different shapes of two-dimensional containers with ‘soft walls,’ where  $\beta$  is the main geometrical parameter linked to the contour’s curvature as

$$\kappa = \frac{2\beta}{(1 + 4\beta^2 y^2)^{3/2}} \quad (2)$$

for  $x > 0$ ,  $-1 < y < 1$ , as  $n \rightarrow \infty$ .

Therefore  $\beta$  is simply one half of the curvature at  $y = 0$ . As mentioned in Introduction, the model (1) enables us to analyze soft analogs of two different types of stiff boundaries. Namely, when  $\beta > 0$ , we have a soft model of billiards with scattering boundaries [13], while the case  $\beta < 0$  gives a soft approximation for the so-called Buminovich stadiums [2]. In our model,  $n$  is a wall stiffness parameter, such that walls become asymptotically stiff as  $n \rightarrow \infty$ . Note that the case of soft walls seems to be more realistic on physical view. Also, soft walls are more convenient from the standpoint of simulations since no conditioning is required for collisions against the walls. Now the model dynamics can be described by the Lagrangian

$$L = \frac{1}{2} \dot{X}^2 - \frac{1}{2} X^2 + \sum_{j=1}^k \left\{ \frac{\mu}{2} \left[ \left( \dot{X} + \dot{x}_j \right)^2 + \dot{y}_j^2 \right] - V_j \right\} \quad (3)$$

where  $V_j = V(x_j, y_j)$  is the potential energy of the  $j$ th particle, and overdots mean differentiation with respect to time  $t$ .

The corresponding Hamiltonian is obtained via the Legendre transform

$$H = P\dot{X} + \sum_{j=1}^k p_j \dot{x}_j - L \quad (4)$$

where  $P = \partial L / \partial \dot{X}$  and  $p_j = \partial L / \partial \dot{x}_j$  are linear momenta.

### III. ANALOGIES WITH BILLIARDS

As follows from bifurcation diagrams obtained for the case of a single particle,  $k = 1$ , the soft wall dynamics are rather dictated by the corresponding billiard shape in rigid-body limit; see Fig.3. Namely, comparing the cases of softer ( $n = 2$ ) and stiffer ( $n = 5$ ) walls, illustrated by the fragments (a) and (b), respectively, shows qualitatively similar dynamic behaviors in similar intervals of the parameter  $\beta$ . The analogy with billiard dynamics is supported by different shapes of trajectories, obtained even with stiffer walls ( $n = 10$ ); see Figs.4 and 5. As seen from Fig.4, container contours and the corresponding trajectories of the particle can take quite different shapes through the interval  $-0.5 < \beta < 0.4$ . In particular, the particle path is either quite regular or chaotic depends upon the number  $\beta$ ; compare to the bifurcation diagrams shown in Fig.3. When

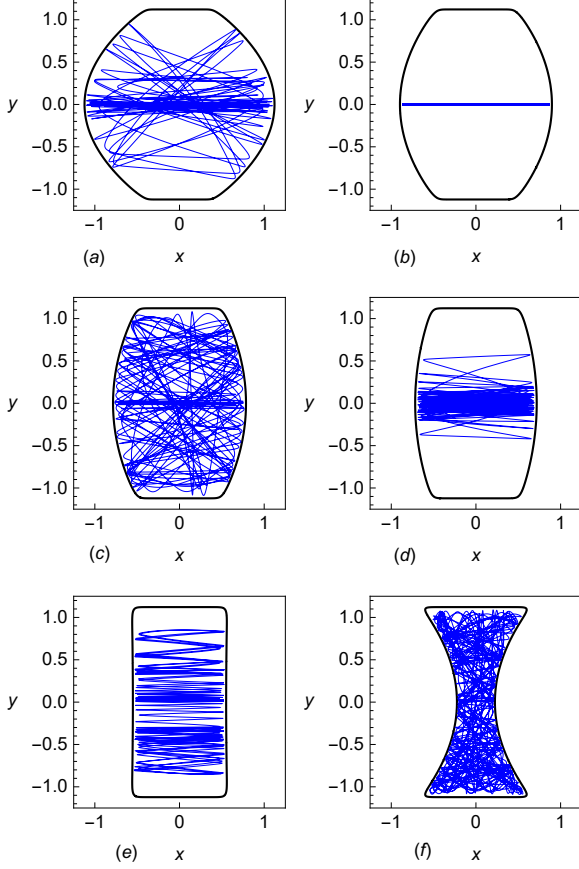


FIG. 4. Trajectories of the particle inside the potential container in the short-term interval  $0 \leq t/T \leq 100$  at  $\alpha = 1/2$ ,  $\gamma = 1.0$ ,  $n = 10$ , and different contour shapes: a)  $\beta = -0.5$ , b)  $\beta = -0.3$ , c)  $\beta = -0.2$ , d)  $\beta = -0.14$ , e)  $\beta = 0.009$ , and f)  $\beta = 0.3$ ; in all cases, the initial position of particle is  $(x, y) = (0.0, 0.01)$  with zero velocity.

contours possess convexities towards the inner domain ( $\beta > 0$ ), the presence of irregularities comes of no surprise due to instabilities caused by the scattering effects. The case  $\beta < 0$  appears to be more complicated since both chaotic and regular motions are possible

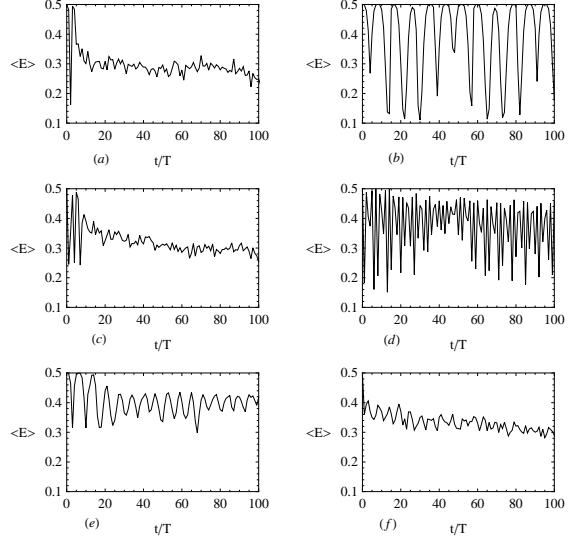


FIG. 5. Time histories of the oscillator's energy corresponding to different contour shapes in Fig. 4;  $\langle E \rangle$  is a mean value over the ensemble of 50 runs with random initial positions of the particle in the domain  $\{-0.01 < x(0) < 0.01, -0.01 < y(0) < 0.01\}$ ; the parameters are  $n = 10$ ,  $k = 1$ ,  $\alpha = 1/2$ .

in different intervals of the curvature. A geometrical nature of such phenomena is likely similar to that was revealed in the case of Buminovich stadia [2], in which the exponential divergence of orbits is possible without convex scatters.

As follows from the above remarks, a possible approach to explanation of regular and chaotic behaviors of the particle may employ transition to the rigid-body billiard limit  $n \rightarrow \infty$ . In this case, the analysis can be conducted in a purely geometrical however quite

complicated way including conditioning dictated by the billiard's stiff boundaries. Alternatively, we use the nonlinear normal modes (NNMs) stability concept [14] with the analytical tool of Floquet theory.

#### IV. NNM'S INSTABILITY AND STOCHASTICITY

In the case of a single particle,  $k = 1$ , there is a NNM whose trajectory is described by the equation  $y_1 = 0$  as dictated by the symmetry of potential well. Although such a trajectory can be only observed under specific initial conditions, its local stability properties appear to have a global effect on the dynamics inside the well. In order to confirm such an observation, let us linearize the model with respect to the coordinate  $y_1$  and re-scale the coordinates and time as

$$\{\bar{x}, \bar{y}, \bar{X}, \bar{t}\} = \frac{1}{\alpha - \beta} \left\{ x, y_1, X, t \sqrt{\frac{\gamma}{\mu}} \right\} \quad (5)$$

As follows from Fig.1 and definition (1), the number  $\alpha - \beta$  becomes the least distance from the origin to a 'vertical' potential wall along the horizontal axis in the rigid-body limit  $n \rightarrow \infty$ . Now let us skip the overbars in notations (5) and consider the differential equations of motion of the particle inside the

potential container

$$\ddot{x} + x^{2n-1} = \frac{\mu}{1 + \mu} \left[ \ddot{x} + \frac{(\alpha - \beta)^2}{\gamma} X \right] \quad (6)$$

$$\ddot{y} + \lambda x^{2n} y = 0 \quad (7)$$

where  $\lambda = -2\beta(\alpha - \beta)$ .

Using the assumption  $\mu \ll 1$  and ignoring the right-hand side of equation (6) gives an unloaded essentially nonlinear oscillator with the power-form characteristic. Such oscillators were considered by Lyapunov when analyzing the degenerated case of his stability of motions theory [7]. The period is calculated through the well tabulated gamma-function  $\Gamma$  as

$$\begin{aligned} T_n &= \frac{4\sqrt{n}}{A_0^{n-1}} \int_0^1 \frac{dz}{\sqrt{1 - z^{2n}}} \\ &= \frac{2}{A_0^{n-1}} \sqrt{\frac{\pi}{n}} \frac{\Gamma(1/(2n))}{\Gamma((1+n)/(2n))} \end{aligned} \quad (8)$$

where  $A_0 = (2nE_n)^{1/(2n)}$  is the amplitude versus the total energy  $E_n = \dot{x}^2/2 + x^{2n}/(2n)$ .

Although different versions of special functions have been suggested to describe the temporal shape of vibrations  $x(t)$ , we prefer to use an approximate solution in terms of elementary functions incorporating the asymptotic of large exponents with a reasonable, for the present case, precision. Such an approximation is obtained in the form of power series expansion with respect to the periodic triangle wave function

$$\tau = \tau \left( \frac{t}{T_n} \right) = \frac{2}{\pi} \arcsin \sin \frac{2\pi t}{T_n}, \quad |\tau| \leq 1 \quad (9)$$

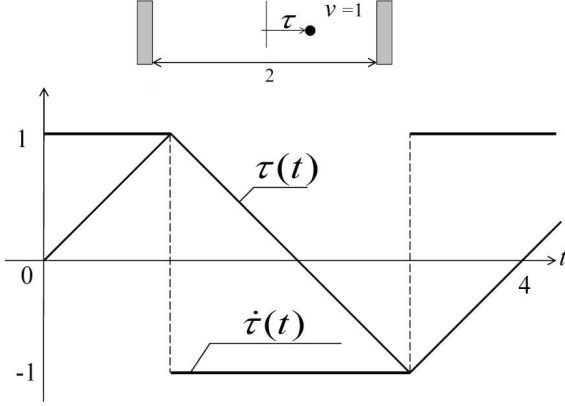


FIG. 6. Vibro-impact oscillator and its dynamic state functions; the relationship  $\dot{\tau}^2 = 1$  holds almost everywhere, therefore  $\dot{\tau}$  can be viewed as a unipotent of the so-called hyperbolic (Clifford's) algebra.

A physical interpretation of function (9) is explained in Fig.6. Namely, we use the dynamic states of elementary vibro-impact oscillator as a basis for the description of non-smooth as well as smooth vibrations based on the fact that the set  $\{1, \dot{\tau}\}$  generates the so-called hyperbolic algebraic structures [11]. A starting point of the corresponding analytical procedure is the periodic temporal substitution  $t \rightarrow \tau$ . This leads to a boundary value problem in the standard interval,  $-1 \leq \tau \leq 1$ , which is solved iteratively to give  $T_n$ -periodic solution

$$x = U(\tau) = A \left( \tau - \frac{\tau^{2n+1}}{2n+1} - R_2 - \dots \right) \quad (10)$$

where the constant parameter  $A$  and the amplitude  $A_0$  are coupled by the equation  $A_0 =$

$U(1)$ , and the following quantities provide estimates for high-order terms of the successive approximations:

$$R_2(\tau, n) = \frac{1}{2} \frac{2n-1}{2n+1} \left( \frac{\tau^{2n+1}}{2n+1} - \frac{\tau^{4n+1}}{4n+1} \right)$$

$$0 < R_i < \frac{(2n-1)|\tau|^{2n+1}}{2^{i-1}(2n+1)^2} \quad (11)$$

In particular, expressions (11) indicate that series (10) converge quite slowly. However, the asymptotic of large exponents essentially improves precision of the truncated series even though first few terms of the series are included. Obviously, as  $n \rightarrow \infty$ , the oscillator becomes a particle between two perfectly stiff barriers  $x = \pm 1$ ; see the upper fragment in Fig. 6.

Due to periodicity of solution (10), equation (7) represents Hill's equation. Note that, compared to the solution  $x(t)$ , the period of the coefficient is reduced as many as twice due to the even exponent  $2n$ . Nonetheless, the period  $T_n$  still leads to the same stability conditions determined by Floquet multipliers  $\rho_{1,2} = \phi \pm \sqrt{\phi^2 - 1}$ . The number  $\phi = [y_1(T_n) + y_2(T_n)]/2$  is calculated through the two fundamental solutions of equation (7),  $y_1(t)$  and  $y_2(t)$ , such that  $y_1(0) = 1$ ,  $\dot{y}_1(0) = 0$  and  $y_2(0) = 0$ ,  $\dot{y}_2(0) = 1$ , respectively. Based on the number  $\phi$ , the solution  $y(t)$  is unstable if  $\phi^2 > 1$ , and stable if  $\phi^2 < 1$ . If  $\phi^2 = 1$ , there exist a periodic solution of equation (7). Fig.7 illus-

trates the dependence  $\phi = \phi(\beta)$ , which actually shows how the curvature of potential contour (2) affects stability of the NNM  $y = 0$ . In particular, stability domains appear to be in a reasonable compliance with those captured with bifurcation diagrams in Fig.3(a), and (b). The relatively narrow instability regions inside the stability intervals are rather caused by the boundary  $\phi = -1$  touched by the curves  $\phi = \phi(\beta)$ ; compare Fig.3 to Fig.7. Note that the bifurcation diagrams impose no conditions on the coordinate  $y$ , whereas the Floquet stability analysis is justified locally, near the axis of symmetry  $y = 0$ . In addition, ignoring the right-hand side of equation (6) is equivalent to a fixed potential container, whereas the bifurcation diagrams in Fig.3 were obtained with the oscillating container. Since both results are nevertheless in match, we can expect that the local stability properties of the NNM  $y = 0$  determine qualitative features of the global dynamics of entire system (3).

## V. RECURRENCE AND DISSIPATIVE EFFECTS

Assuming that the main oscillator of mass  $M$  is given some initial energy, while the inner particles are in rest, we analyze the process of energy transfer from the oscillator to the particles at different magnitudes of the

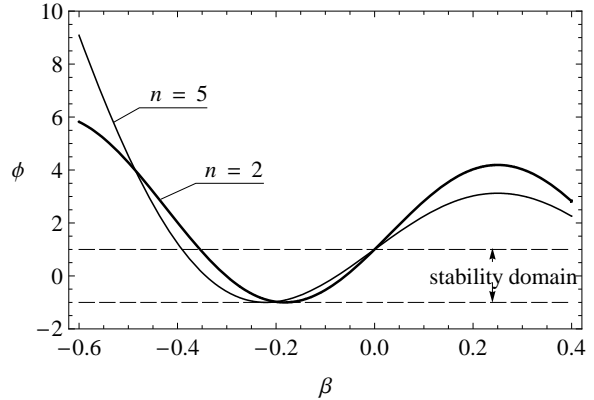


FIG. 7. The stability domain.

parameter  $\beta$ . Since the model (3) is conservative then both the direct and reversed energy flows are possible. However, the energy exchange dynamics look different in different intervals of the parameter  $\beta$  as confirmed already by Figs.4 and 5, where different fragments of Fig.5 relate to the same cases in Fig.4. In order to eliminate the possible influence of initial conditions, we consider the mean energy flow over ensembles of randomly taken initial positions of the particle in a narrow area near zero. It is seen that the trend of the energy outflow from the donor is associated with the stochastic behavior of the receiver, and it may take place in both negative and positive unstable sub intervals of the parameter  $\beta$ .

Below we analyze long-term trends of the energy flow by increasing the observation interval to 1500 eigen periods of the oscillator,  $0 \leq t/T \leq 1500$ . Consider first the case of scattering convex potential,  $\beta = 0.3$ . The

result of simulations, which is represented in Fig.8, confirms the presence of energy outflow effect at different however still small number non-interacting particles inside the potential container. Recall that the total mass of the energy absorbing particles remains fixed as  $m = k\mu = 0.2$ . However, it is seen that the effect becomes more explicit as the number of particles is increasing from  $k = 1$  to  $k = 5$ .

In addition to the direct visualization of the energy's time histories, we use a convenient tool of recurrence plots [4], [10]; see the upper fragments in Fig.9. A recurrence plot depicts the collection of pairs of times at which the trajectory crosses the same  $\varepsilon$ -neighborhood of the system phase space. In particular, defining the distance in terms of energies, the recurrence (or non-recurrence) can be characterized by the binary function defined on the two-dimensional integer grid as

$$R(i, j) = \begin{cases} 1, & |E_i - E_j| \leq \varepsilon \\ 0, & \text{otherwise} \end{cases} \quad (12)$$

where the energy snapshots  $E_k = E(kT)$  are taken at every period of the main oscillator  $T = 2\pi$ .

In the coordinate plane  $i - j$ , ones are shown with colors, whereas zeros remain white; see for instance the corresponding fragments in Fig. 9. According to the definition (12), all the recurrence plots are symmetric with respect to the diagonal  $i =$

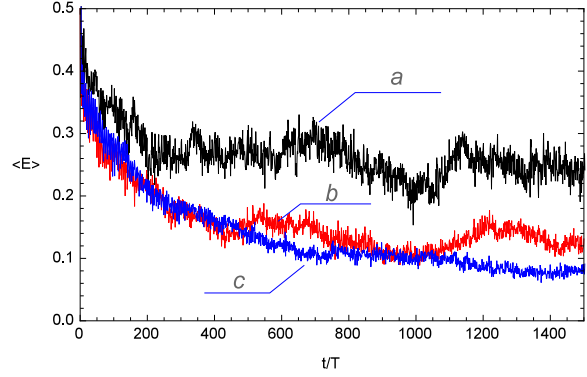


FIG. 8. Container's energy during the temporal interval  $0 \leq t/T \leq 1500$  in the case of convex scatters ( $\beta = 0.3$ ) with the following numbers of particles: a)  $k = 1$ , b)  $k = 3$ , and c)  $k = 5$ ; the averaging is taken over ensemble of 25 runs over random initial positions of particles in the domain  $\{-0.01 < x(0) < 0.01, -0.01 < y(0) < 0.01\}$ .

$j$ , on which  $|E_i - E_j| = 0$ , and therefore  $R(i, j) = 1$  for any  $i = j$ . A non-diagonal point  $(i, j)$  associates the recurrence time as  $t_{rec} = T|i - j|$ . Note that frequent collisions of small particles against potential walls produce short-term fluctuations of the energy  $E$  generating a relatively narrow cloud of points near the diagonal  $i = j$  with very short recurrence times. From the standpoint of long-term trends, however, the meaningful points should distance from the diagonal in such a way that the longer trend is of interest the longer distance must be considered.

As already mentioned, Fig.8 illustrates long-term temporal behaviors of the mean en-

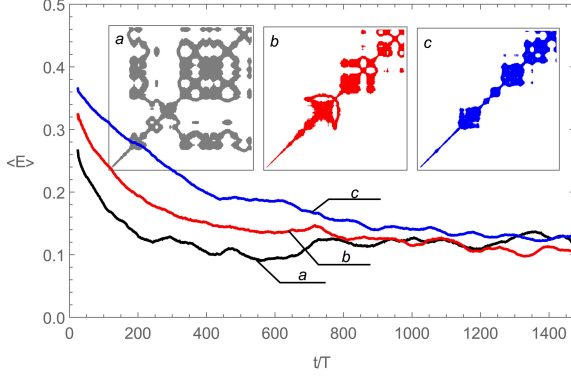


FIG. 9. The running  $50T$  average of the container's energy with recurrence diagrams for different container's shapes: a)  $\beta = -0.5$ , b)  $\beta = -0.2$ , and c)  $\beta = 0.3$ ; the horizontal and vertical axes of recurrence diagrams cover the intervals  $0 \leq i, j \leq 1500$ ; the number of particles and wall stiffness parameter are fixed as  $k = 3$  and  $n = 4$ , respectively.

ergy  $\langle E \rangle$  at different numbers of particles inside the container. In all the cases, the initial energy is  $E = 1/2$ . Since all the particles are initially in rest, the energy of main oscillator  $\langle E \rangle$  always drops quite abruptly, when the potential wall first collides with the particle(s). However, further energy behaviors are dictated by the number of particles and the parameter  $\beta$ . In particular, the long-term energy decay is developing more clearly as the number of particles increases. Further, Fig. 9 shows time histories with the corresponding recurrence plots of the mean energy  $\langle E \rangle$  at different positive and negative magnitudes of the parameter  $\beta$ . Although all of the num-

bers  $\beta$  belong to the NNM instability intervals, the instability develops in different rates due to different Floquet multipliers. Note that some recurrence effects are observed in the case of Buminovich type potential contour; see the case (a) in Fig.9. This can be explained more clearly by comparing plots in Fig.9(a), (b), and (c) with trajectories of the particle inside potential wells shown in Fig. 4(a), (c), and (f), respectively. Obviously, in the case (a),  $\beta = -0.5$ , the trajectory is less chaotic, therefore some recurrence effects can be expected.

## VI. GENERALIZATIONS

Let us modify the potential function as

$$V = \frac{\gamma}{2n} \left[ \left( \frac{x}{\alpha + \beta(y^2 - 1)} \right)^{2n} + \left( \frac{y}{\alpha + \beta(x^2 - 1)} \right)^{2n} \right] \quad (13)$$

Compared to (1) the potential well (1) is symmetric  $x \rightleftharpoons y$ . For instance, if  $\beta > 0$  then all the four pieces of contour's boundary are convex scatters; see Fig.10. Qualitatively, the corresponding bifurcation diagram, which is shown in Fig. 11, is similar to the previous case of flat horizontal boundaries; compare to Fig. 3. However, there are some numerical differences. For example, the number  $\beta = 1.0$  belongs now to the unstable

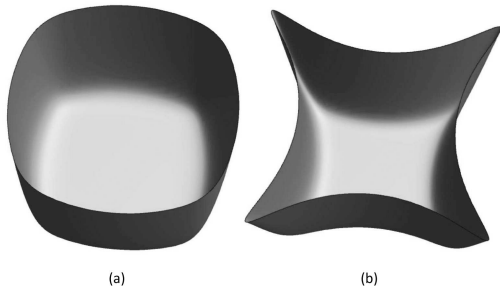


FIG. 10. Potential well shapes: a)  $\beta = -0.1$ -stadium type well, and b)  $\beta = 0.1$ -convex scattering walls;  $\alpha = 1.0$ ,  $\gamma = 1.0$ ,  $n = 6$ .

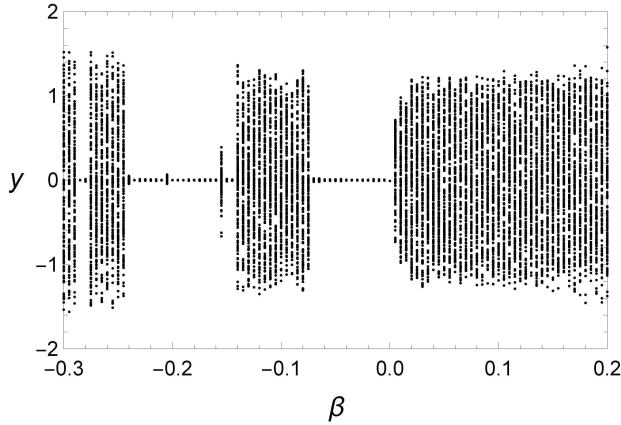


FIG. 11. Bifurcation diagram for the case of a single particle,  $k = 1$ , inside the symmetric potential well (13) obtained with parameters:  $\alpha = 1.0$ ,  $\gamma = 1.0$ ,  $n = 6$ .

domain. Therefore, both the potential wells shown in Fig. 10 generate the stochastic dynamics, and therefore the energy absorbing property of inner particles.

The result of simulation for the case of convex scatters,  $\beta = 0.1$ , is illustrated in Fig. 12. In particular, it shows that the ‘statistical equilibrium’ at about  $\langle E \rangle = 0.1$  is reached

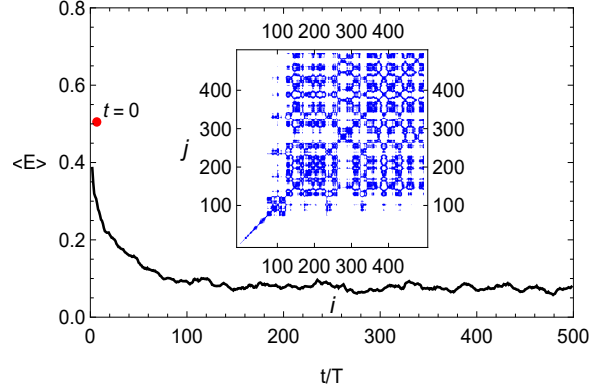


FIG. 12. Simulation results in the case of five particles,  $k = 5$ , with the potential well parameters:  $\alpha = 1.0$ ,  $\gamma = 1.0$ ,  $n = 6$ , and  $\beta = 1.0$ ; the averaging is taken over the ensemble of 25 runs and then processed with five periods,  $5T$ , running average; the initial energy of the container,  $\langle E \rangle = 0.5$  is shown by the dot  $t = 0$ .

after approximately 100 vibration cycles of the container. Then the total container energy is fluctuating near the value  $\langle E \rangle = 0.1$  with quite small amplitudes; see both the time history and the recurrence plot in Fig. 12. Therefore particles inside the symmetric container appear to absorb the energy more effectively compared to the case of flat boundaries (1).

## VII. CONCLUSIONS

Analyses of the suggested model revealed the existence of effective ‘energy sinks’ in low-dimensional Hamiltonian systems with potential wells whose contours, in the rigid-

body limit, can take different shapes resembling the so-called Sinai and Bunimovich billiards. We found that the energy flow shows the one-directional trend during a reasonably long time in the eigen temporal scale of the system. The analogy with billiards combined with the nonlinear normal modes stability concept allowed us to determine such parameter intervals in which light particles inside the potential container possess the energy absorbing property. On macro-levels, the suggested model can be used for the design of energy absorbing (harvesting) devices. This can be done by making container shapes sim-

ilar to the potential contours revealed in the present work. Periodic arrays of nano-cells with different types of ‘stochastic shapes’ can be considered as well in order to design new energy absorbing materials. In reality, the effect of energy absorption will be enhanced due to inelastic collisions of particles with container walls. On molecular levels, different ‘potential containers’ can be created by heavier particles of crystal lattices with arrays of lighter inclusions. For instance, the repulsive component of Lennard-Jones potential, considered on layers of cubic lattices, can have shapes similar to that shown in Fig.10(b).

- 
- [1] S. Aubry, G. Kopidakis, A.M. Morgante, and G.P. Tsironis. Analytic conditions for targeted energy transfer between nonlinear oscillators or discrete breathers. *Physica B: Condensed Matter*, 296(1-3):222 – 236, 2001. Proceedings of the Symposium on Wave Propagation and Electronic Structure in Disordered Systems.
  - [2] L. A. Bunimovich. Decay of correlations in dynamical systems with chaotic behavior. *Sov. Phys. JETP*, 62:842–852, 1985.
  - [3] F. Cottone, H. Vocca, and L. Gammaitoni. Nonlinear energy harvesting. *Phys. Rev. Lett.*, 102:080601, Feb 2009.
  - [4] J.-P. Eckmann, S. Oliffson Kamphorst, and D. Ruelle. Recurrence plots of dynamical systems. *EPL (Europhysics Letters)*, 4(9):973, 1987.
  - [5] L. Gammaitoni, I. Neri, and H. Vocca. Nonlinear oscillators for vibration energy harvesting. *Applied Physics Letters*, 94(16), 2009.
  - [6] C. Jarzynski. Energy diffusion in a chaotic adiabatic billiard gas. *Phys. Rev. E*, 48:4340–4350, Dec 1993.
  - [7] A.M. Liapunov. *Stability of Motion by A M Liapunov*. Mathematics in Science and Engineering. Elsevier Science, 2000.
  - [8] R.S. MacKay, L. Vázquez, M.P. Zorzano, and M.P. Zorzano. *Localization and Energy Transfer in Nonlinear Systems*. World Scientific, 2003.

- [9] P. Maniadis and S. Aubry. Targeted energy transfer by fermi resonance. *Physica D: Nonlinear Phenomena*, 202(3-4):200 – 217, 2005.
- [10] N. Marwan. A historical review of recurrence plots. *The European Physical Journal Special Topics*, 164(1):3–12, 2008.
- [11] V. N. Pilipchuk. *Nonlinear Dynamics: Between Linear and Impact Limits (Lecture Notes in Applied and Computational Mechanics)*. Springer, 2010.
- [12] A B Ryabov and A Loskutov. Time-dependent focusing billiards and macroscopic realization of maxwell’s demon. *Journal of Physics A: Mathematical and Theoretical*, 43(12):125104, 2010.
- [13] Y. G. Sinai. Dynamical systems with elastic reflections: ergodic properties of dispersing billiards. *Russian Math. Surveys*, 25:137–189, 1970.
- [14] A. F. Vakakis, L. I. Manevitch, Yu. V. Mikhlin, V. N. Pilipchuk, and A. A. Zevin. *Normal modes and localization in nonlinear systems*. John Wiley & Sons Inc., New York, 1996. A Wiley-Interscience Publication.
- [15] A.F. Vakakis, O.V. Gendelman, L.A. Bergman, D.M. McFarland, G. Kerschen, and Y.S. Lee. *Nonlinear Targeted Energy Transfer in Mechanical and Structural Systems*. Springer-Verlag, Berlin Heidelberg, 2009.
- [16] N. J. Zabusky and M. D. Kruskal. Interaction of ”solitons” in a collisionless plasma and the recurrence of initial states. *Phys. Rev. Lett.*, 15:240–243, Aug 1965.
- [17] G. M. Zaslavskii and B. V. Chirikov. Stochastic instability of non-linear oscillations. *Physics-Uspekhi*, 14(5):549–568, 1972.
- [18] R. Zwanzig. Nonlinear generalized langevin equations. *Journal of Statistical Physics*, 9(3):215–220, 1973.